

Lattice thermal conductivity: A comparison of molecular dynamics and anharmonic lattice dynamics

102

Anthony J. C. Ladd and Bill Moran

Lawrence Livermore National Laboratory, University of California, P.O. Box 808, Livermore, California 94550

William G. Hoover

*Lawrence Livermore National Laboratory, University of California, P.O. Box 808, Livermore, California 94550
and Department of Applied Science, University of California at Davis—Livermore, Livermore, California 94550*

(Received 2 June 1986)

The thermal conductivity of a monatomic face-centered-cubic lattice has been calculated over a range of temperatures from one-twentieth to one-half the melting temperature. An inverse-twelfth-power "soft-sphere" potential was used to represent the interatomic forces. We have examined, quantitatively, the approximations involved in deriving the Peierls phonon-transport expression for the thermal conductivity and have determined the temperature range over which it is useful. This has involved extensive comparisons with the formally exact Green-Kubo method, using molecular dynamics to generate the phase-space trajectories. At low temperatures, the relaxation processes in a crystal can be described in terms of phonon lifetimes. We have calculated the lifetimes of all the phonon states of 108-, 256-, and 864-particle classical crystals, with periodic boundaries, by molecular dynamics and by anharmonic perturbation theory. These lifetimes were then used to estimate the thermal conductivity.

I. INTRODUCTION

The thermodynamic and transport properties of anharmonic crystals are generally described in terms of the interactions between phonons.¹ The anharmonic forces cause the phonon spectrum to shift and broaden, so that the normal-mode amplitudes are no longer purely periodic functions of time. If the anharmonic interaction is small, so that the lifetime of a phonon state is many vibrational periods, the normal-mode amplitudes can be written as²

$$Q(t) = Qe^{-i(\omega + \Delta - i\Gamma)t}, \quad (1.1)$$

where ω is the unperturbed harmonic frequency, and Δ and Γ are the frequency shift and linewidth. These line shifts and linewidths depend on the thermodynamic state of the crystal and can be measured by a variety of experimental techniques, of which the most powerful is neutron scattering.³ A comparison of theoretical and experimental line shapes provides a detailed check on proposed intermolecular forces.

Transport properties of solids can be estimated from the phonon lifetimes,⁴ which we define by

$$\tau = \frac{\int_0^\infty \langle \delta n(t) \delta n(0) \rangle dt}{\langle (\delta n)^2 \rangle}, \quad (1.2)$$

where n , proportional to Q^*Q , is the phonon occupation number, and δn indicates the fluctuation of n from its equilibrium value. It can be seen that the lifetime and linewidth are simply related

$$\tau = (2\Gamma)^{-1}. \quad (1.3)$$

Despite the fact that there are well-known formulas,

both classical and quantum, for the phonon line shifts and linewidths,¹⁻³ they have never been evaluated for enough normal modes to enable a definitive calculation of the thermal conductivity to be made. Calculations of phonon line shapes are generally restricted to a few symmetry directions.^{3,5,6} Analytic estimates for the thermal conductivity, obtained by approximating the Brillouin-zone sums,^{7,8} differ by more than 50% for the inverse-twelfth-power potential.

A formally exact method of relating transport coefficients to the decay of fluctuations in microscopic fluxes has been described by Green and Kubo.⁹ Numerical results from molecular-dynamics simulations are available for fluids of particles interacting with hard¹⁰ and soft¹¹ forces. The molecular-dynamics method is not restricted to small amplitude displacements of the particles. It is therefore ideal for investigating deviations from the inverse temperature dependence of the thermal conductivity, λ , predicted by classical phonon perturbation theory.^{4,7,8} In the first part of this work, we compare the autocorrelation function and resulting thermal conductivity derived from the exact microscopic heat flux,¹² with the approximate formulation, valid only at low temperatures in terms of phonon energies and group velocities.^{4,13} This enables us to determine the range of validity of the Peierls expression for the thermal conductivity as a function of temperature or rms displacement.

We have calculated, from our molecular dynamics simulations, the coefficient, $\lim_{T \rightarrow 0} (\lambda T)$ that describes the low-temperature thermal conductivity of classical crystals. This can be compared with theoretical calculations based on the Peierls theory of thermal conduction.^{4,13} We have compared our molecular-dynamics-based result with approximate theories,^{7,8} and more rigorous estimates based

on calculating phonon lifetimes for all the normal modes of finite-size crystals and extrapolating to the thermodynamic limit. The phonon lifetimes were calculated by molecular dynamics and anharmonic perturbation theory.

The calculations described in this work were carried out for a monatomic face-centered-cubic crystal. The interparticle forces were derived from a pairwise-additive inverse-twelfth-power potential,

$$\phi(r) = \epsilon(\sigma/r)^{12} \quad (1.4)$$

truncated beyond the second neighbors. For this potential, there exists a corresponding states principle linking thermodynamic or hydrodynamic states described by the same dimensionless parameter

$$x = (N\sigma^3/\sqrt{2}V)(\epsilon/k_B T)^{1/4}.$$

For instance, the scaled thermal conductivity $\lambda T^{-2/3}$ is a function of x only.¹⁴ For ease of comparison with theoretical results we ignore this scaling and treat ϵ and σ as independent variables. The reduced density $N\sigma^3/\sqrt{2}V$ is equal to unity throughout this work, and the melting temperature at this density, T_m , is $2.29\epsilon/k_B$.¹⁴

II. HEAT FLUX AND THERMAL CONDUCTIVITY

A general expression for the thermal conductivity, first derived by Green and Kubo has now been obtained in many different ways.⁹ The conductivity λ is related to the decay of equilibrium fluctuations of the microscopic heat current, q ,

$$\lambda = \frac{V}{k_B T^2} \int_0^\infty \langle q_x(t) q_x(0) \rangle dt, \quad (2.1)$$

where V is the volume, T is the temperature, and k_B is Boltzmann's constant. We will indicate how the expression for the thermal conductivity of crystalline solids derived by Peierls,^{4,13} can be obtained from the Green-Kubo expression under certain approximations, valid at low temperature.

For a classical system of point masses, interacting via pairwise-additive forces, a microscopic expression for the heat flux has been derived by Irving and Kirkwood,¹² assuming that half the pair interaction energy can be associated with each particle. If the temperature gradient is slowly varying over a distance corresponding to the range of interparticle forces, then the heat flux is independent of any reasonable method of localizing the potential energy. Irving and Kirkwood's prescription leads to an expression for the heat flux q in terms of the relative coordinates, r_{mn} , and forces, F_{mn} , between pairs of particles, and the individual particle velocities v_m ,

$$qV = \frac{1}{2} \sum_m m v_m^2 v_m + \frac{1}{2} \sum_{m>n} [\phi_{mn}(v_m + v_n) + F_{mn} \cdot (v_m + v_n) r_{mn}]. \quad (2.2)$$

This expression can also be derived, in an analogous

way to the momentum flux or pressure tensor, from the "heat theorem,"¹⁵

$$\frac{d}{dt} \sum_m r_m e_m = 0, \quad (2.3)$$

where e_m is the energy associated with particle m . Since there is negligible macroscopic particle diffusion in a crystalline solid, and since small fluctuations in the particle coordinates cannot cause energy transfer over macroscopic distances and times, the heat theorem for a solid is simply

$$\sum_m \overline{r_m^0} \dot{e}_m = 0, \quad (2.4)$$

where r_m^0 indicates the average coordinate of particle m . This leads to an alternative and simpler expression for the heat current

$$qV = \frac{1}{2} \sum_{m>n} (v_m + v_n) \cdot F_{mn} r_{mn}^0. \quad (2.5)$$

Similar expressions have been derived for the pressure and elastic constants.¹⁶ It should be noted that no assumption of small displacements is made in deriving Eq. (2.5); only the absence of particle diffusion is required. Numerical checks have shown that thermal conductivities obtained using Eq. (2.5) are identical to those obtained using Eq. (2.2) though the instantaneous ($t=0$) current fluctuations are different.

If the interparticle potential is expanded in a power series in the relative displacements, u_{mn} , the first nonvanishing contribution to the heat flux, quadratic in the displacements is, from Eq. (2.5),

$$q^0 V = -\frac{1}{2} \sum_{m>n} r_{mn}^0 [u_{mn}(\dot{u}_m + \dot{u}_n) : (\nabla \nabla \phi_{mn})_{r_{mn}=r_{mn}^0}], \quad (2.6)$$

where $\nabla \nabla \phi_{mn}$ is the force-constant matrix, and r_{mn}^0 is the average separation vector. Thermal conductivities calculated with this heat flux are strictly valid only at low temperatures.

If the particle displacements are expanded in a set of normal modes with amplitude Q and polarization ϵ , then for a crystal of N atoms of mass m , with a fixed center of mass, enclosed by periodic boundaries,

$$u_m = (mN)^{-1/2} \sum_i Q_i \epsilon_i e^{ik_i \cdot r_m^0}, \quad (2.7)$$

where the sum is over the discrete set of $(N-1)$ vectors and three branches contained in the first Brillouin zone. It is then straightforward to show that the approximate expression for the heat flux in Eq. (2.6) is equivalent to the formula first derived by Peierls,^{4,13}

$$q^p V = \sum_i n_i \omega_i v_i, \quad (2.8)$$

where ω_i and v_i are the frequency and group velocity and n_i , which has units of action, is related to the usual definition of the phonon occupation number, n_{occ} ,

ts and
nough
of the
homon
me
nduc-
-zone
elfth-
oeffi-
luxes
al re-
lable
of 11
icted
It is
e in-
vity,
4,7,8
rela-
ived
oxi-
rms
bles
res-
am-
ics
the
ds.
ed
ve
p-
ed
y

$$n = (n_{\text{occ}} + \frac{1}{2})\hbar = m\omega Q^* Q. \quad (2.9)$$

This definition makes for a simple correspondence between quantum and classical results, since the energy associated with a particular mode is $n\omega$ in both cases. In Sec. IV we compare numerical results for the thermal conductivity using the three expressions for the heat flux q , q^0 , and q^p .

The Peierls expression for thermal conductivity^{4,13} is a simplification of the Green-Kubo result, obtained by substituting the approximate phonon heat flux, q^p , with the result

$$\lambda^{\text{Pe}} = \frac{1}{3Vk_B T^2} \sum_{i,i'} \omega_i \omega_{i'} v_i \cdot v_{i'} \int_0^\infty \langle n_i(t) n_{i'}(0) \rangle dt. \quad (2.10)$$

Since the ensemble-averaged heat current is zero, we can replace the occupation numbers by their fluctuations, δn_i . If the correlation between different phonon states $\langle n_i(t) n_{i'}(0) \rangle$ is ignored, then the conductivity can be written in the form derived by Peierls¹³

$$\lambda^{\text{Pe}} = \frac{k_B}{3V} \sum_i v_i^2 \tau_i \quad (2.11)$$

which follows from the definition of the phonon lifetime (1.2) and the classical thermodynamic fluctuation formula $\langle (\delta n_i)^2 \rangle = (k_B T / \omega_i)^2$.

III. THERMAL CONDUCTIVITY: NUMERICAL RESULTS

We have calculated by molecular dynamics the thermal conductivity for the inverse-twelfth-power potential over a range of temperatures up to about one-half the melting temperature, with two goals in mind. First we wished to find the coefficient of the inverse temperature dependence that characterizes the low-temperature thermal conductivity of classical crystals. Second we wished to determine deviations from the low-temperature T^{-1} behavior caused by higher-order anharmonicities. These deviations occur in the heat current itself, beginning with terms proportional to the third derivative of the potential, and in the dynamics, beginning with linear terms proportional to the sixth derivative of the potential together with terms involving products of lower-order derivatives. Although both types of deviation must be included simultaneously for a systematic expansion of the conductivity in powers of the temperature, it is of theoretical interest to examine them separately. We compare thermal conductivities obtained using the exact microscopic heat flux q , with those obtained from the quadratic approximations to the heat flux q^0 and q^p .

Heat flux autocorrelation functions were obtained at temperatures $(k_B T / \epsilon)$ near 0.1, 0.2, 0.5, and 1.0 for crystals sizes from 108 to 864 particles. The correlation functions were averaged over run times of 600–10 000 $(m\sigma^2/\epsilon)^{1/2}$ (after equilibration) or about 2400–40 000 Einstein (single-particle) vibrational periods. The classical equations of motion were numerically integrated by an ordinary differential equation solver¹⁷ which maintained the energy conservation to about $10^{-4} N k_B T$. The phonon occupation numbers, used in calculating the phonon heat

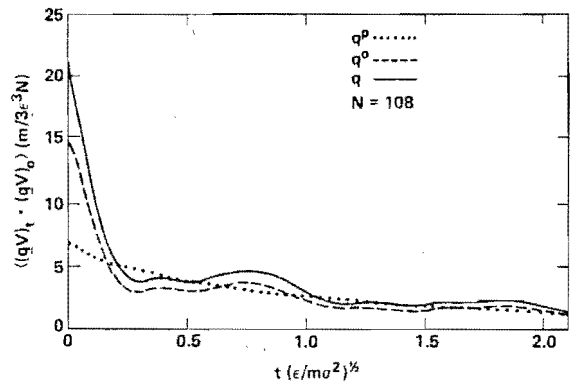


FIG. 1. Heat flux autocorrelation functions of q , q^0 , and q^p for $N=108$ and $T=0.546\epsilon/k_B$. Only the initial portions of the correlation functions are shown.

flux q^p were obtained by a spatial Fourier analysis of the instantaneous particle coordinates and velocities.

Heat flux autocorrelation functions are illustrated in Fig. 1 at a temperature $k_B T / \epsilon = 0.55$. The atomistic representations of the heat flux, (2.2) and (2.6), result in oscillatory correlation functions, caused by the rapid transport of energy back and forth over microscopic distances, by the atomic vibrations of the lattice. These fluctuations are averaged out by transforming to a phonon basis, resulting in a monotonic decay of the heat current, as might be expected macroscopically. In fact, the phonon heat flux correlation function $\langle q^p(t) \cdot q^p(0) \rangle$ neatly bisects its atomic counterpart $\langle q^0(t) \cdot q^0(0) \rangle$, and the integrals of these two correlation functions are identical within the statistical errors. The atomistic correlation functions have a similar time dependence; the major anharmonic contribution to the conductivity coming from the larger instantaneous fluctuations of the exact heat flux, $\langle q \cdot q \rangle$.

The average long-time decay of these correlation functions can be most easily seen in the phonon heat flux correlation function which is shown at the two extreme temperatures in Fig. 2 for $N=108$ and 256. At high temperatures, there is little difference between the correlation functions for $N=108$ and 256, but at low temperatures, heat currents persist much longer in the smaller system. This is due to the reduced number of phonon scattering mechanisms.

The various estimates of the thermal conductivity are shown in Table I. We see that the Green-Kubo molecular-dynamics method is an effective route to the thermal conductivity of classical crystals even at low temperatures. Run times of $1000(m\sigma^2/\epsilon)^{1/2}$ were usually sufficient to reduce the statistical errors to less than 10%. The number dependence of the thermal conductivity arises from the different long-time decay rates of the heat flux autocorrelation functions (Fig. 2), and is surprisingly small. Although the thermal conductivities obtained with $N=108$ and 256 are significantly different at low temperatures, the conductivities for $N=256$ and 864 are similar. This small number dependence is probably due to two canceling effects. As the crystal gets larger, lower frequency phonons, which generally make significant con-

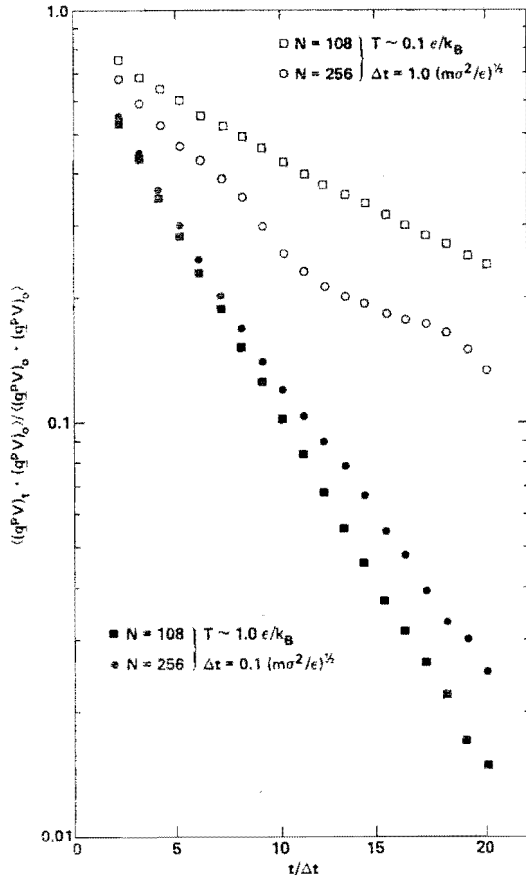


FIG. 2. Long-time behavior of the normalized phonon heat flux correlation functions at approximate temperatures of 0.1 and $1\epsilon/k_B$. A comparison of results for $N=108$ and 256 is shown.

tributions to the conductivity, are permitted. On the other hand, the increased number of scattering possibilities decreases the phonon lifetimes.

Nonequilibrium molecular-dynamics simulations of thermal conduction using hot and cold reservoirs were found to be impractical for three-dimensional crystals.¹⁸

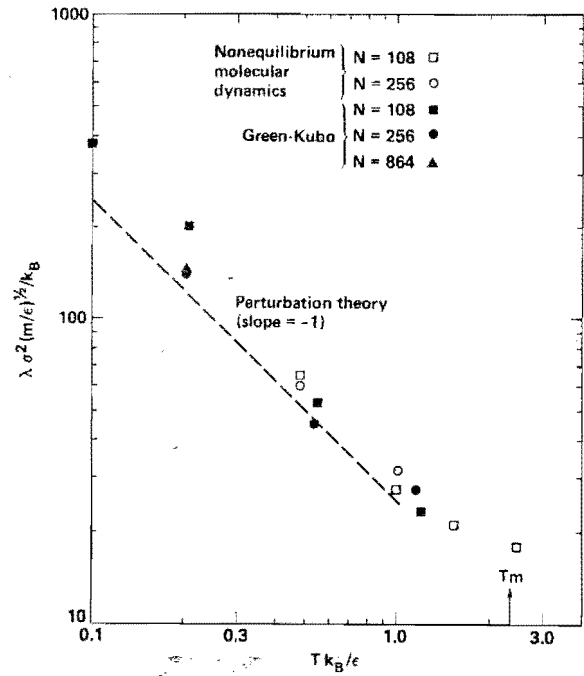


FIG. 3. Thermal conductivity from equilibrium Green-Kubo, nonequilibrium molecular dynamics, and phonon perturbation theory. The melting temperature is indicated by the vertical arrow labeled T_m .

The phonon scattering was dominated by boundary effects. Homogeneous nonequilibrium simulations worked much better and conductivities could be obtained with about 10% accuracy for the high-temperature solid phase.¹⁴ These results, together with some more recent nonequilibrium simulations, are compared with the equilibrium Green-Kubo results in Fig. 3. This comparison indicates that the two methods calculate similar thermal conductivities, though the nonequilibrium method is less precise because the conductivity does not vary in any simple way with the external field used to simulate a temperature gradient.

The thermal conductivities derived from the harmonic

TABLE I. Thermal conductivity of classical face-centered-cubic crystals interacting via an inverse-twelfth-power potential. The thermal conductivities derived from each heat flux are shown together with the temperature and run time t_r . The statistical errors are estimated to be about 5% for $N=108$, 10% for $N=256$, and 15% for $N=864$. $\lambda^* = \lambda \sigma^2 (m/\epsilon)^{1/2} / k_B$.

Tk_B/ϵ	N	$t_r(\epsilon/m\sigma^2)^{1/2}$	λ^*	$(\lambda^0)^*$	$(\lambda^p)^*$	λ^0/λ
0.103	108	10 000	380	360	365	0.95
0.101	256	1000			280	
0.208	108	10 000	203	181	180	0.89
0.205	256	1000	140	125		0.89
0.204	864	600	150	135		0.90
0.546	108	8000	53.2	41.7	41.4	0.78
0.534	256	900	45	36		0.80
1.191	108	5000	23.2	14.4	13.4	0.62
1.142	256	1000	27.7	16.7	16.0	0.60

heat fluxes q^0 and q^p are in agreement with each other, and vary as T^{-1} at low temperatures. Our best estimate of the coefficient $\lim_{T \rightarrow 0}(\lambda^0 T)$ is $26 \pm 1(\epsilon^3/m\sigma^4)^{1/2}$. Theoretical estimates of the thermal conductivity have been given by Julian⁷ and Klemens.⁸ Julian calculates the Brillouin zone sums that occur in the Peierls formula in an approximate way, and for the inverse-twelfth-power potential predicts that $\lambda^0 T = 44(\epsilon^3/m\sigma^4)^{1/2}$. Klemens's theory, based on the Debye model, is in much better agreement with our molecular-dynamics results and gives a value of $\lambda^0 T = 28(\epsilon^3/m\sigma^4)^{1/2}$. We have also calculated this coefficient from first principles, using the Peierls formula (2.11), and lifetimes determined from phonon perturbation theory (see Sec. IV). The result $\lambda^0 T = 25(\epsilon^3/m\sigma^4)^{1/2}$, is in good agreement with our molecular-dynamics data (see Fig. 3).

At high temperatures, $T > 0.5\epsilon/k_B$, the conductivities λ^0 and λ^p , calculated using quadratic approximations to the heat flux decay more rapidly than T^{-1} , due to the effect of higher-order anharmonicities on the phonon lifetimes. However, if anharmonic contributions to the heat flux are included, the conductivity λ falls off as approximately T^{-1} up to temperatures of $1\epsilon/k_B$. It can be seen in Fig. 3 that the thermal conductivity λ follows the low-temperature perturbation theory prediction over this range of temperatures. Beyond a temperature of $1\epsilon/k_B$ the conductivity decreases more slowly than T^{-1} . The ratio λ^0/λ is about 0.6 at $k_B T/\epsilon = 1$. These results suggest that extensions of the low-temperature Peierls theory for the thermal conductivity should include the higher-order displacement contributions to the heat flux and dynamics simultaneously.

IV. PHONON LIFETIMES

We can calculate phonon lifetimes from Eq. (1.2) using the phonon occupation numbers obtained by Fourier analyzing the instantaneous particle displacements and velocities. At low enough temperatures we expect to make contact with classical phonon perturbation theory. We have calculated phonon lifetimes for 108 and 256 atom crystals at four temperatures between 0.1 and $1.0\epsilon/k_B$. We estimate that the statistical errors in the phonon lifetimes are between 10 and 30%. A harmonic phonon basis was used, and the thermal conductivities obtained using the Peierls formula (2.8) agree with our Green-Kubo results for λ^0 and λ^p . Of course, at high temperatures these conductivities are considerably smaller than the "exact" result, λ .

Phonon lifetimes calculated by molecular dynamics exhibit a complex dependence on the magnitude and direction of the wave vector \mathbf{k} . As an example, phonon lifetimes in the [100] and [110] directions are shown in Fig. 4, as a function of the magnitude of \mathbf{k} . The boundaries of the first Brillouin zone are at $k\sigma = \sqrt{2}\pi$ and $k\sigma = 3\pi/2$ for the [100] and [110] directions, respectively. A [110] phonon lying outside the first Brillouin zone with $k\sigma = 2\pi$ is equivalent to a zone-boundary [100] phonon, $k\sigma = \sqrt{2}\pi$. The longitudinal and in-plane transverse modes of the [110] phonon form the degenerate transverse modes of the [100] phonon and the out-of-plane trans-

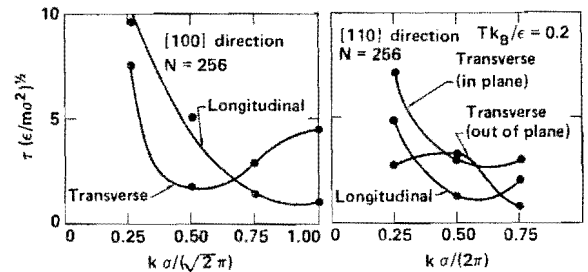


FIG. 4. Phonon lifetimes as a function of k in the [100] and [110] directions, for $N=256$ and $T=0.2\epsilon/k_B$. The solid lines are drawn as a visual aid to identify the various branches. In the [110] direction the two transverse modes are not degenerate and have different frequencies for motion in the plane of the k vector and perpendicular to this plane.

verse [110] mode becomes the longitudinal [100] mode. The lifetimes shown in Fig. 4 are consistent with this symmetry.

The temperature dependence of the phonon lifetimes is illustrated in Fig. 5 again for [100] and [110] phonons. At low temperatures, the lifetimes are proportional to T^{-1} as expected from classical phonon perturbation theory. This inverse temperature dependence characterizes the lifetimes of long-wavelength phonons over the temperature range we have studied. However, the lifetimes of higher- k phonons fall off more rapidly than

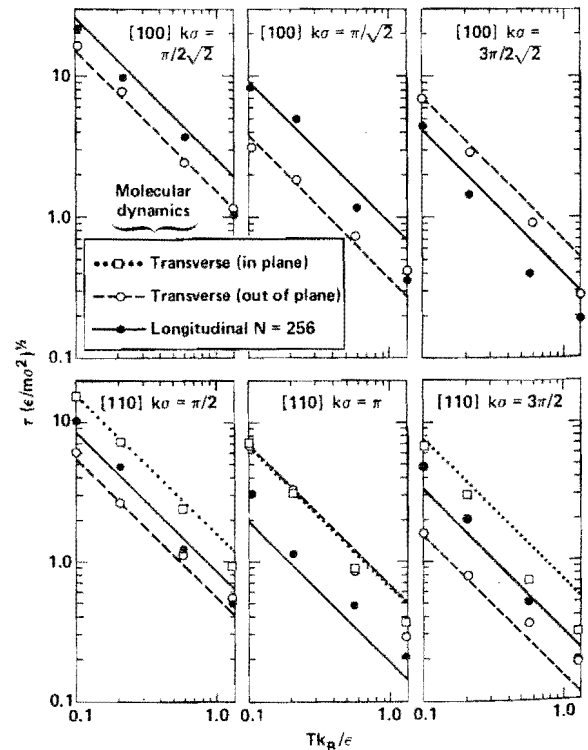


FIG. 5. Temperature dependence of the phonon lifetimes, in the [100] and [110] directions for $N=256$ at various values of k . The solid lines are the results of anharmonic perturbation theory for $N=256$.

It is not possible to quantify these deviations with the available statistics.

The straight lines, with a slope of -1 , in Fig. 5 are the predictions of classical phonon perturbation^{1,3} theory for $N=256$. The frequency shifts and linewidths were calculated from the usual perturbation-theory expressions,^{1,3} and the lifetime was obtained from the linewidth via Eq. (2.1). In applying anharmonic perturbation theory to the calculation of frequency shifts and linewidths, we have used the conventional representations of the delta function and principal value^{3,5}

$$\delta(\omega) = \lim_{\Delta\omega \rightarrow 0^+} \frac{1}{\pi} \frac{\Delta\omega}{\omega^2 + (\Delta\omega)^2}, \quad (4.1)$$

$$\left[\frac{1}{\omega} \right]_p = \lim_{\Delta\omega \rightarrow 0^+} \frac{\omega}{\omega^2 + (\Delta\omega)^2},$$

and the problem reduces to choosing an appropriate value of $\Delta\omega$, corresponding to a smearing out of the harmonic phonon reference spectrum, which is a sequence of delta functions at the phonon frequencies. If $\Delta\omega$ is too large, the details of the phonon spectrum are washed out; if $\Delta\omega$ is too small, there is very little overlap between adjacent phonon states. An alternative method,⁶ involving analytic integration over small regions of the Brillouin zone, is not applicable to finite-size crystals.

We have found empirically that a narrow range of values of $\Delta\omega$, of the order of $0.05 (\epsilon/m\sigma^2)^{1/2}$, brings the perturbation theory and molecular-dynamics results for both $N=108$ and 256 into quite good agreement, especially considering the statistical uncertainties in the molecular-dynamics results. A suitable criterion for choosing $\Delta\omega$ turns out to be minimizing the sum of the squares of the frequency shifts, which corresponds in a general way to the least sensitive choice of $\Delta\omega$. The perturbation theory results shown in Figs. 3 and 5 adopt this criterion.

The predictions of classical perturbation theory can be assessed in an overall way by comparing the thermal conductivity calculated via the Peierls formula, Eq. (2.11), using the perturbation-theory lifetimes, with the molecular-dynamics results for the conductivities λ^0 or λ^p . These results are shown in Table II together with the appropriate $\Delta\omega$ found by minimizing the variation in the frequency shifts, and the sensitivity of the conductivity to the choice

of $\Delta\omega$. It can be seen that the molecular-dynamics and perturbation-theory results are in good agreement for the larger crystals, and that $\Delta\omega$ is steadily decreasing with increasing N , as is the sensitivity of the conductivity to the choice of $\Delta\omega$. These results suggest that we have found a useful procedure for applying phonon perturbation theory to finite-size crystals.

It would be desirable from both theoretical and numerical standpoints to develop a theory that does not require these empirical manipulations. Since anharmonic interactions can bring a crystal of almost any size to thermodynamic equilibrium, theories that require a continuous phonon spectrum are incomplete. Numerical work on lattice vibrations would be greatly assisted if direct perturbation-theory methods for calculating phonon lifetimes in finite-size crystals were available.

V. CONCLUSIONS

The equilibrium Green-Kubo method is currently the most effective route to the thermal conductivity of classical crystals, and can be applied over a wide range of temperatures. Long runs are necessary to obtain good statistics, but this is compensated for by the weak number dependence; a few hundred particles are sufficient for temperatures down to one-tenth of the melting temperature. Nonequilibrium molecular dynamics works poorly at low temperatures, but is consistent with Green-Kubo at temperatures greater than one-half melting.

At low temperatures the Green-Kubo results are in agreement with phonon perturbation theory. At one-half melting, the Peierls calculation of the conductivity gives about one-half the correct value; the remainder is accounted for by contributions of higher-order displacements, cubic and beyond to the heat flux. However, higher-order anharmonicities cause the phonon lifetimes to decay more rapidly than T^{-1} , and the net effect is that the conductivity can be characterized by an inverse temperature dependence up to about one-half melting. The coefficient of the inverse temperature dependence is quite accurately predicted by Klemens's theory,⁸ but not by Julian's.⁷

A difficulty arises in applying anharmonic perturbation-theory calculations to finite-size crystals. The harmonic reference spectrum must be smeared out to cause some overlap between adjacent phonon states. We have found a simple empirical rule for assigning a width

TABLE II. Low-temperature thermal conductivity. The slope of the classical T^{-1} dependence of the conductivity is calculated by molecular dynamics (MD) and perturbation theory (PT). The molecular-dynamics results are derived from the Green-Kubo calculations using the quadratic approximation to the heat flux, q^0 . The empirical width of the reference phonon spectrum used in the perturbation theory is shown together with the sensitivity of the conductivity to the choice of $\Delta\omega$. The highest normal-mode frequency in the crystal is about $35(\epsilon/m\sigma^2)^{1/2}$.

N	$(\lambda^0 T)_{MD} (m\sigma^4/\epsilon^3)^{1/2}$	$(\lambda^{Pe} T)_{PT} (m\sigma^4/\epsilon^3)^{1/2}$	$\Delta\omega (m\sigma^2/\epsilon)^{1/2}$	$\frac{\partial(\lambda^{Pe} T)_{PT}}{\partial(\Delta\omega)\sigma^{-1}\epsilon}$
108	36	27.2	0.80	8
256	25	25.6	0.55	9
364	27	25.3	0.25	4

to the harmonic spectrum which brings lattice dynamics and molecular-dynamics calculations of phonon lifetimes into good agreement with each other. It also leads to a series of thermal conductivities that converges quite quickly with increasing crystal size. It would be interesting to develop a perturbation theory that could be directly applied to finite-size crystals, without the use of *ad hoc* prescriptions.

ACKNOWLEDGMENTS

We are pleased to acknowledge helpful discussions with Alex Maradudin (University of California, Irvine) and Mike Klein (National Research Council of Canada). This work was supported by the U.S. Department of Energy and Lawrence Livermore National Laboratory under Contract No. W-7405-Eng-48.

-
- ¹J. A. Reissland, *Physics of Phonons* (Wiley, London, 1973); P. Choquard, *The Anharmonic Crystal* (Benjamin, New York, 1967).
- ²D. C. Wallace, *Thermodynamics of Crystals* (Wiley, New York, 1972).
- ³A. A. Maradudin and A. E. Fein, *Phys. Rev.* **128**, 2589 (1962).
- ⁴P. G. Klemens, in *Solid State Physics*, edited by F. Seitz and D. Turnbull (Academic, New York, 1958), Vol. 7.
- ⁵R. A. Cowley, *Rep. Prog. Phys.* **31**, 123 (1968); L. Böhlin and T. Högberg, *J. Phys. Chem. Solids* **29**, 1805 (1968).
- ⁶V. V. Goldman, G. K. Horton, T. H. Keil, and M. L. Klein, *J. Phys. C* **3**, L33 (1970).
- ⁷C. L. Julian, *Phys. Rev.* **137**, A128 (1965).
- ⁸P. G. Klemens, *High Temp.—High Pressures* **15**, 249 (1983).
- ⁹R. W. Zwanzig, *Ann. Rev. Phys. Chem.* **16**, 67 (1965).
- ¹⁰B. J. Alder, D. M. Gass, and T. E. Wainwright, *J. Chem. Phys.* **53**, 3813 (1970).
- ¹¹D. Levesque, L. Verlet, and J. Kärkijärvi, *Phys. Rev. A* **7**, 1690 (1973).
- ¹²J. H. Irving and J. G. Kirkwood, *J. Chem. Phys.* **18**, 817 (1950).
- ¹³R. E. Peierls, *Ann. Phys.* **3**, 1055 (1929).
- ¹⁴W. G. Hoover, B. Moran, and J. M. Haile, *J. Stat. Phys.* **37**, 109 (1984).
- ¹⁵W. G. Hoover, B. Moran, R. M. More, and A. J. C. Ladd, *Phys. Rev. A* **24**, 2109 (1981).
- ¹⁶W. G. Hoover and Z. W. Salzburg, *J. Chem. Phys.* **54**, 2129 (1971).
- ¹⁷A. C. Hindmarsh, *Association for Computing Machinery Signum Newsletter* **15**, 10 (1980).
- ¹⁸R. D. Mountain and R. A. MacDonald, *Phys. Rev. B* **28**, 3022 (1983).